Journal of Catalysis **185,** 307–313 (1999)
Article ID jcat.1999.2495, available online at http://www.idealibrary.com on IDEAL®

Gas Phase Transesterification of Dimethylcarbonate and Phenol over Supported Titanium Dioxide

Won Bae Kim and Jae Sung Lee[1]

Department of Chemical Engineering/School of Environmental Engineering, Pohang University of Science and Technology (POSTECH), San 31 Hyoja-dong, Pohang 790-784, Korea

Received September 28, 1998; revised March 8, 1999; accepted March 19, 1999

The transesterification of dimethylcarbonate and phenol has been studied in a continuous gas flow reactor at high temperatures which were found to be favorable thermodynamically for high yields of methylphenylcarbonate (MPC). Among various solid catalysts, TiO_2/SiO_2 showed the highest activity and selectivity for MPC. The structure and the chemical state of titanium species in TiO_2/SiO_2 have been investigated by means of X-ray diffraction (XRD), X-ray photoelectron spectroscopy (XPS), and X-ray absorption near edge structure (XANES) of Ti *K*-edge. It was observed that the titanium species was highly dispersed on silica. Below 10 wt% Ti loading, the titanium phase was not observed by XRD, yet weak XRD peaks of anatase were detected at higher loadings. The Ti *K*-edge XANES spectra and XPS analyses indicated that Ti(IV) species in the form of a monolayer was dominant below 5 wt% Ti loadings and TiO_2 of the anatase structure appeared at higher loadings. The amount of the surface Ti(IV) species measured by XPS increased with Ti loadings and was saturated above 10 wt% in the same manner as the selectivity to MPC changed with Ti loadings. This suggested that surface Ti(IV) species was directly responsible for the selective synthesis of MPC. The crystalline anatase TiO_2 was also an active and selective catalyst for the transesterification, yet it contributed to decrease in activity by coking.

Key Words: **transesterification; gas phase; dimethylcarbonate; phenol; TiO_2/SiO_2; XANES; active phase.**

INTRODUCTION

Polycarbonate has been conventionally produced by the interfacial polycondensation of bisphenol-A and phosgene. Drawbacks of the conventional phosgene process include environmental and safety problems involved in the use of a copious amount of methylenechloride as the solvent, which is 10 times the weight of the products, and a highly toxic phosgene as the reagent (1). Hence, phosgene-free processes for polycarbonate have been proposed that employ melt transesterification (2–5) or solid state polymerization (1, 6) using bisphenol-A and diphenylcarbonate (DPC) with the latter synthesized in a phosgene-free process.

[1] To whom correspondence should be addressed. Fax: 82-562-279-5799. E-mail: jlee@postech.ac.kr.

The fact that environmental costs are an integral part of process economics is having a profound influence on technical developments in the chemical, petroleum refining, and power generation industries. Particularly important is the application of catalytic technologies that result in processes that use fewer toxic raw materials, eliminate by-products that are hazardous and difficult to dispose of, and lower emissions (7).

Diphenylcarbonate, a convenient intermediate for the synthesis of polycarbonate without using phosgene, has often been synthesized via a two-step reaction from dimethylcarbonate (DMC) and phenol (8–11) since the direct synthesis of DPC is limited due to low equilibrium constants for the forward reaction (9). The first step, transesterification of DMC and phenol proceeds as shown in reaction [1] and formed methylphenylcarbonate (MPC) is disproportionated into DPC and DMC in reaction [2]:

$$CH_3O(C{=}O)OCH_3 + C_6H_5OH \rightleftharpoons C_6H_5O(C{=}O)OCH_3 + CH_3OH \quad [1]$$

$$2\,C_6H_5O(C{=}O)OCH_3 \rightleftharpoons C_6H_5O(C{=}O)OC_6H_5 + CH_3O(C{=}O)OCH_3. \quad [2]$$

Usually, the transesterification of DMC and phenol is carried out in the liquid phase using homogeneous catalysts such as organic Pb, Sn, or Ti compounds. Recently, Fu *et al.* (11) reported that molybdenum oxide supported on silica showed the highest activity for both the transesterification and the disproportionation in the liquid phase reaction. This is one of a few reports on the development of active solid catalysts for the reaction. However, there exists a critical thermodynamic limitation for the synthesis of DPC from DMC and phenol, especially in the reaction 1 (9). Tundo *et al.* (12) reported the reaction of DMC with phenol under continuous flow of gaseous reactants over a solid bed supporting a liquid phase-transfer catalyst. A spherical macroporous α-alumina (3 mm in diameter, 0.03 $m^2\,g^{-1}$ surface area) was coated with 5 wt% of potassium carbonate and 5 wt% of PEG 6000 and used as support for the base

0021-9517/99 $30.00

and the catalyst. However, anisole was the sole product. They suggested that the transesterification between DMC and phenol was not favored thermodynamically with K_{eq} of ca. 3×10^{-4} at 453 K (12).

In this work, the transesterification of DMC and phenol (reaction [1]) was performed in a continuous gas flow fixed bed reactor over solid catalysts at high temperatures which were found to be more favorable from the thermodynamic calculation of the reaction [1] (13). Among various catalysts tested, titanium oxide supported on SiO_2 was the most active catalyst for the transesterification of DMC and phenol in the gas phase. The same catalyst was also found to be highly efficient in the disproportionation of MPC in the liquid phase reaction (13, 14). We employed several spectroscopic techniques such as X-ray diffraction (XRD), X-ray photoelectron spectroscopy (XPS), X-ray absorption near edge structure (XANES), and N_2 adsorption to investigate the structure of the active components and the correlation between the structure and the activity of the TiO_2/SiO_2 catalyst in the gas phase transesterification of dimethylcarbonate and phenol.

EXPERIMENTAL

Catalysts Preparation

To prepare TiO_2/SiO_2 catalysts, SiO_2 (Aldrich 23683-7) was impregnated with a solution of tetrabutoxytitanium (Aldrich 24411-2) dissolved in toluene. Samples of different metal loadings given in weight percent by metal were dried in an oven at 383 K for 12 h to remove the organic solvent and calcined in a quartz reactor at 773 K for 4 h with an air stream of 89 μmol s^{-1}.

Gas Phase Transesterification of DMC and Phenol

The catalysts were pretreated under a flow of nitrogen gas at a rate of 15 μmol s^{-1} at 773 K for 1 h just prior to the delivery of the mixture of DMC and phenol. The reactant mixture was a solution of DMC (Aldrich D15292-7) and phenol (Aldrich 18545-0) with a ratio of 5 mol DMC to 1 mol phenol. The reactants were introduced into the flow of nitrogen gas of 15 μmol s^{-1} via a syringe pump (Sage Instruments Model 361) at a pumping rate of 1.0 cm^3 h^{-1} at atmospheric pressure. A vaporization chamber filled with glass beads was positioned upstream of a Pyrex U type reactor to ensure a complete mixing of gaseous reactants. Identification and quantitative analysis of reaction products were carried out by an on-line HP 5890II gas chromatograph (GC) equipped with a flame ionization detector (FID) and by a GC-Mass spectrometer of HP 5890II-HP5972MSD. An HP PONA capillary column (50 m $\times$ 0.2 mm $\times$ 0.5 μm) was used to separate products for GC analysis. A sample was injected into GC every 20 min by a six-port sampling valve attached to the effluent stream line.

Characterization of the TiO_2/SiO_2 Catalyst

The specific surface areas of the catalysts were determined on a constant volume adsorption apparatus (Micrometrics ASAP 2021C surface area analyzer) by the N_2 BET method at the liquid nitrogen temperature. Powder X-ray diffraction (XRD) measurements were conducted on a MAC Science Co. Model M18XHF X-ray diffractometer using a radiation source of Cu $K\alpha$ ($\lambda = 1.5405$ Å) at 40 kV and 200 mA with a scanning rate of 4° min^{-1}. X-ray photoelectron spectroscopy (XPS) measurements were carried out using a Perkin-Elmer PHI 5400ESCA spectrometer with monochromatic Mg $K\alpha$ radiation (1253.6 eV) at 15 kV and 20 mA. The vacuum in the measurement chamber, during the collection of spectra, was maintained below 5×10^{-9} Torr. The pass energy of the measurement was 89.45 eV. Charging effect was circumvented by referencing binding energies to that of C_{1S} peak at 284.6 eV. X-ray absorption near edge structure (XANES) spectra were taken of the *K*-edge of Ti in a transmission mode at beamline 3C1 of the Pohang Accelerator Laboratory (PAL) in Pohang, Korea, operating at 2.0 GeV with ca. 100–150 mA of the stored current. Double-crystal Si(111) monochromators were used for the measurement. The detector gases were N_2 for both the incident and the transmitted beams. The obtained data were analyzed using the UWXAFS 3.0 package licensed from University of Washington. The standard procedure is described in detail elsewhere (15).

RESULTS

Gas Phase Transesterification of DMC and Phenol over TiO_2/SiO_2 Catalysts

In catalyst screening experiments in a fixed bed, continuous gas flow reactor, it was found that the most efficient catalyst was TiO_2 supported on activated carbon or silica (14). The catalyst performed significantly better than MoO_3/SiO_2 which was the catalyst recommended by Fu *et al.* (11) for the liquid phase transesterification of DMC and phenol. Hence, TiO_2/SiO_2 catalyst was chosen for further study and its properties were investigated in more detail in the following. Phenol conversion and selectivity to methylphenylcarbonate (MPC) was determined at a time on stream of ca. 8.5 h when a steady state reaction was established. The MPC selectivity (%) is defined as the moles of MPC produced per 100 mole of consumed phenol and MPC yield (%) is obtained from multiplication of phenol conversion by MPC selectivity.

It was observed that the major by-products were anisole and cresol, which could be produced via methylation of phenol with DMC. Generally, more anisole was formed than cresol by a few times with all catalysts through a nucleophilic attack of methyl group in DMC by the phenoxy compound. However, little diphenylcarbonate (DPC) was

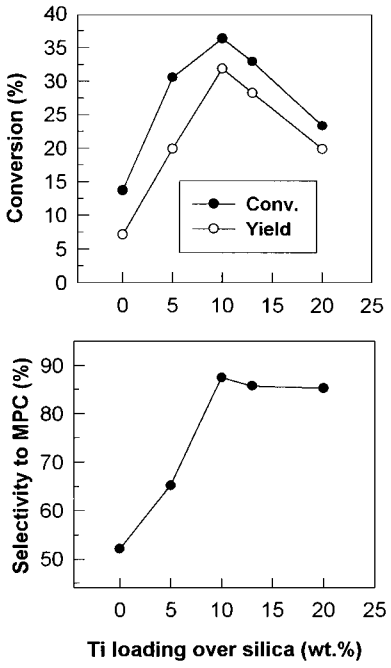

FIG. 1. The activities at steady state for the transesterification of DMC and phenol as a function of weight percentage of titanium loaded. Reactant mixture feeding rate, 1.0 $cm^3 h^{-1}$; mole ratio of DMC to phenol, 5; N_2 flow rate, 15 μmol s^{-1}; TiO_2/SiO_2 catalyst loading, 0.48 g; reaction temperature, 703 K.

produced, indicating that there was an insufficient contact time for the consecutive transesterification of MPC with phenol to occur. It was found that the production of DPC became appreciable as the space velocity of reactants decreased further.

Gas phase reactivity of DMC over TiO_2/SiO_2 catalysts was more complicated than that of liquid phase as discussed elsewhere (16). When gas phase DMC itself is supplied, without phenol over TiO_2/SiO_2, dimethylether, methanol, CO_2, and carbon deposit were produced. At the initial stage of the transesterification of DMC and phenol, DMC was rapidly and completely converted to dimethylether, methanol, CO_2, and carbon deposit as in the case without phenol. At the steady state of the reaction, however, most of converted DMC reacted with phenol to produce MPC and by-products such as anisole and cresol while very little DMC converted to dimethylether. Overall, the MPC selectivity based on DMC was more than 90% at the steady state in all cases.

We carried out a preliminary study on the effects of reaction variables on the performance of the catalysts and a part of the results including temperature effects were reported elsewhere (14). Briefly, the conversion of phenol increased with increasing temperature below 703 K, but it showed a much slower increase above 703 K. The selectivity for MPC did not show much variation with reaction temperatures of 640–750 K and remained at $86 \pm 5\%$. Hence, we chose 703 K as our standard reaction temperature. The phenol conversion increased continuously as the concentration of DMC in the feed was increased at a fixed phenol feed. However, MPC selectivity showed a maximum at DMC/phenol ratio of 5 and this ratio became a standard reaction condition.

Figure 1 shows the steady state activities of the transesterification reaction at 703 K as a function of weight percentage of titanium in TiO_2/SiO_2 catalysts. The conversion of phenol and the yield of MPC both showed maxima at 10 wt% Ti loading. The selectivity toward MPC increased with Ti loading up to 10 wt% and remained constant at about 87% with higher Ti loadings. It should be noted that silica itself (points at 0% Ti loading) had appreciable activity, yet selectivity was low at about 52%.

X-ray Diffraction

The structure and the chemical state of titanium oxide species on silica have been investigated by means of several spectroscopic methods such as X-ray diffraction, X-ray photoelectron spectroscopy, and X-ray absorption fine structure. Figure 2A shows the results of X-ray diffraction (XRD) analyses for the fresh TiO_2/SiO_2 catalysts with different Ti loadings. At low Ti loadings, the titanium phase was not observed. Weak, but characteristic peaks of anatase type TiO_2 were detected for TiO_2/SiO_2 catalysts with Ti loadings greater than 10 wt%. The used catalysts showed

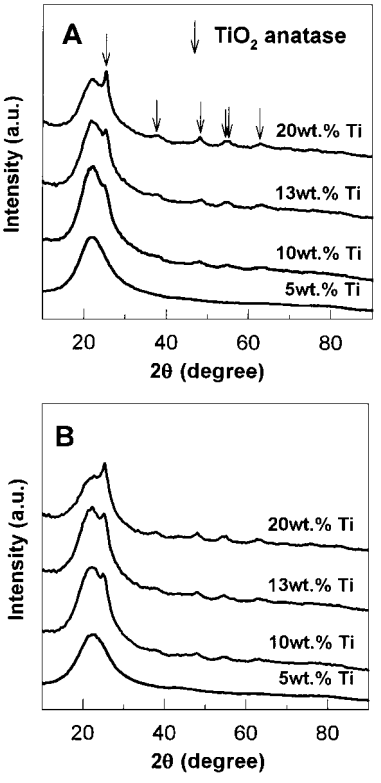

FIG. 2. X-ray diffraction patterns of TiO_2/SiO_2 catalysts with the different Ti loadings before (A) and after the reaction (B) at 703 K for 8.5 h.

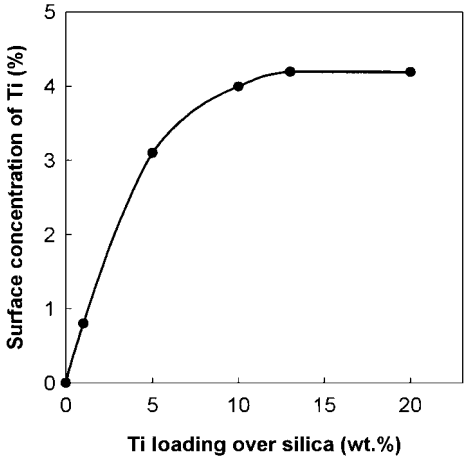

FIG. 3. The surface concentration of Ti as a function of Ti loading in TiO_2/SiO_2 before reaction determined from XPS quantitative analyses.

exactly the same patterns of XRD as shown in Fig. 2B, implying that the sintering of catalyst during the reaction had not occurred.

X-ray Photoelectron Spectroscopy

The investigation of binding energy and intensity of some surface elements by X-ray photoelectron spectroscopy (XPS) gives the information of the chemical states and relative quantities of the outermost surface compounds. The Ti $2p_{3/2}$ binding energies of the TiO_2/SiO_2 catalysts were invariant with Ti loading in the range of 458.3 ± 0.2, which corresponds to the binding energy of titanium dioxide. Binding energies of Ti $2p_{3/2}$ electrons are 454.0 ± 0.2, 455.0 ± 0.2, and 458.8 ± 0.3 eV for titanium metal, titanium monoxide, and titanium dioxide, respectively.

Figure 3 represents the Ti atomic concentration obtained from quantitative XPS analyses of the outermost surface of TiO_2/SiO_2 catalysts as the weight percentage of Ti is increased. The surface concentration of Ti increased rapidly up to 5 wt% Ti. Between 5 and 10 wt% Ti, the surface concentration increased at a slower rate. Above 10 wt% the surface concentration of Ti reached a constant value of 4.2%. This result indicates the mode of TiO_2 dispersion on the support as Ti loading is raised. Below 5 wt%, TiO_2 is highly dispersed probably as monolayer, but in higher loadings it begins to be crystallized into bulk titania. Especially above 10 wt% Ti, further added titania contributes to the growth of crystal phase, but not to the dispersion of titania on the silica surface. The surface compositions (%) of other components measured by XPS with different Ti loadings are as follows in the order of O, Si, and C: 70.4, 25.6, and 3.2 for 1 wt% catalyst, 67.4, 23.2, and 6.3 for 5 wt% catalyst, 68.1, 24.2, and 3.6 for 10 wt% catalyst, 67.7, 21.1, and 6.9 for 13 wt% catalyst, and 66.5, 18.6, and 10.7 for 20 wt% TiO_2/SiO_2 catalyst. As Ti loading increased, surface concentration of Si decreased while that of carbon increased.

X-ray Absorption Near Edge Structure

X-ray absorption near edge structure (XANES) is a powerful tool used to investigate the local structure around an absorbing atom. For this reason the coordination state of Ti has often been probed by XANES at the Ti *K*-edge. Ti(IV) is in a d^0 configuration corresponding to A_1 or A_{1g} states depending on tetrahedral or octahedral symmetry (17). The first feature in XANES of Ti *K*-edge is the pre-edge corresponding to the excitation of 1*s* electrons into empty bound states derived from the *d* and *p* states of Ti and O atoms. In tetrahedral symmetry, since the final states are T_2 and E, the transitions of A_1 into T_2 and E occur. As considerable mixing of 3*d* and 4*p* orbitals occurs, the A_1-into-T_2 transition is allowed and the corresponding pre-edge peak became particularly strong. This transition overwhelms the weaker A_1-into-E transition and therefore tetrahedral symmetry of Ti(IV) shows a strong single peak in the pre-edge region. In the case of octahedral symmetry, the transition of 1*s* electrons occurs into empty *d* orbitals and the final states are T_{2g} and E_g. Hence, expected transitions are A_{1g}-into-T_{2g} and A_{1g}-into-E_g, which are both Laporte forbidden. Consequently, the octahedral symmetry of Ti(IV) shows weaker pre-egde absorption peaks than that for the tetrahedral symmetry. Usually, three weak peaks are observed. Two of them are associated with A_{1g}-into-T_{2g} and A_{1g}-into-E_g transitions as described above. The third peak, which is at the lowest energy, is of uncertain origin. Analyses of XANES around the Ti *K*-edge are presented here, comparing the spectra of the catalysts with those of reference compounds.

Figure 4 shows the XANES spectra of reference Ti compounds, namely titanium metal, anatase type and rutile type

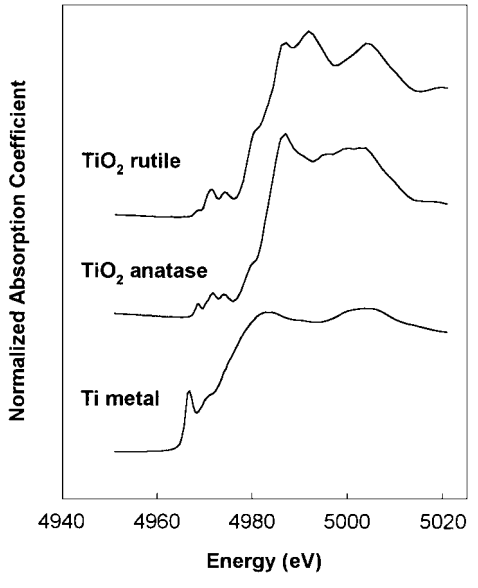

FIG. 4. X-ray absorption near edge structures (XANES) of Ti *K*-edge for reference Ti compounds.

titania. The pre-edge peak of Ti metal was very sharp and high. The high and single peak in the pre-edge region indicates that the Ti in the metal has a tetrahedral symmetry. However, this spectrum of Ti(0) species could be differentiated from that of tetrahedral Ti(IV) species which shows similar pre-edge peak shape but its absorption edge is observed at a higher energy. Anatase and rutile showed three weak pre-edge peaks, indicating an octahedral symmetry. In the post-edge region, the resonance patterns of the absorption coefficient for anatase and rutile titania are somewhat different. The resonances present in the rutile phase derived from constructive interference at ca. 4992 eV and ca. 5020 eV were not present in anatase.

Figure 5 represents Ti *K*-edge XANES spectra of TiO_2/SiO_2 catalysts with different Ti loadings. In pre-edge region, only 5 wt% catalyst showed a single peak although it is not as sharp as typical tetrahedral Ti(IV) species (17, 18). Thus, 5 wt% TiO_2/SiO_2 catalyst appears to contain both tetrahedral Ti(IV) species and octahedral Ti(IV) species. Catalysts with higher Ti loadings ($\geq$10 wt%) showed the pre-edge feature of typical octahedral symmetry. In post-edge region of spectra, the characteristic peaks of rutile type titania were not observed, such as resonance peaks at 4992 and 5020 eV, indicating titanium oxide species on silica were Ti(IV) dioxide of anatase form. With increasing Ti loadings, the peak intensity increased, especially that at ca. 5004 eV. This feature of XANES spectra indicates that the crystallinity of titania is augmented as Ti loading is increased above 10 wt% of Ti.

Specific Surface Area

Figure 6 illustrates change in specific surface area for TiO_2/SiO_2 catalysts at increasing Ti loadings before and after the reaction. The fresh TiO_2/SiO_2 catalysts showed

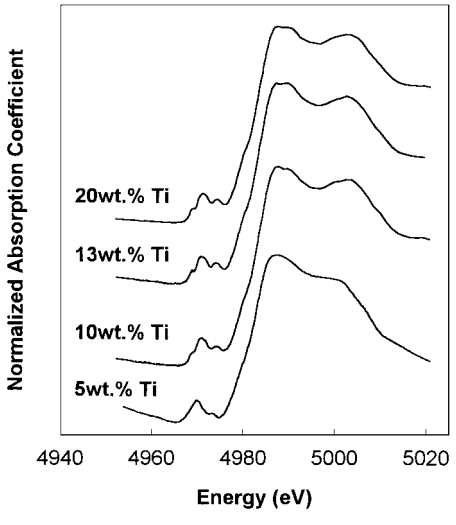

FIG. 5. X-ray absorption near edge structures (XANES) of Ti *K*-edge for the TiO_2/SiO_2 catalysts as a function of Ti loading.

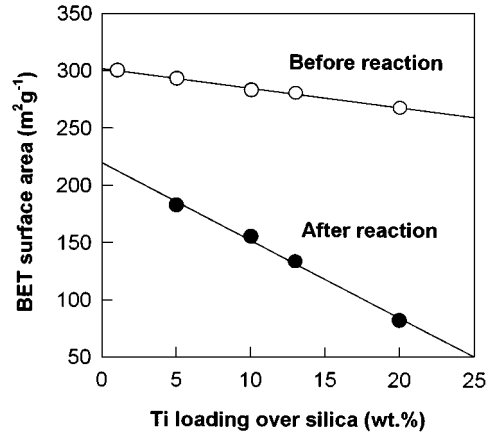

FIG. 6. BET surface area of the TiO_2/SiO_2 catalysts as a function of Ti loading before and after reaction at 703 K for 8.5 h.

an almost linear decrease of BET areas as Ti content increased up to 20 wt%. The slope was very small and change was within 10% for whole Ti loadings. However, the used catalysts showed a more rapid decline of specific surface area as Ti loading was increased. Thus, the surface area difference of the fresh and the used catalysts was greater for higher Ti content.

DISCUSSION

In this work, a new method for the synthesis of diphenylcarbonate (DPC) from dimethylcarbonate (DMC) and phenol was proposed. Methylphenylcarbonate (MPC) is the inevitable intermediate in the synthesis of DPC from DMC and phenol, but is difficult to be produced in a high yield through the conventional liquid phase reaction due to the low thermodynamic equilibrium constants. By using the functional group contribution method (19), the standard heat of reaction [1] in the gas phase was estimated to be 23.5 kJ mol^{-1} (13). Equilibrium yields of this endothermic reaction should be more favorable as reaction temperature increases. In this new scheme, TiO_2/SiO_2 was found to be an efficient catalyst, giving a higher yield of MPC in a fixed bed gas flow reactor at a relatively high temperature. DPC could be obtained effectively through the liquid phase disproportionation of MPC over the same catalyst (13). In the present work, we investigated the structure and chemical state of the active components of the TiO_2/SiO_2 catalyst system and their relationship with catalytic activity in the gas phase transesterification of dimethylcarbonate and phenol.

There are a large number of studies in the literature on the structure of supported TiO_2. Stranick *et al.* (20) employed XPS, XRD, and laser Raman spectroscopy (LRS) to characterize the dispersion and chemical state of titanium in a series of TiO_2/Al_2O_3 catalysts. Titania was well dispersed on alumina for Ti loadings less than 14 wt%. The formation

of a TiO_2 : Al_2O_3 surface phase occurred in 1 to 6 wt% Ti range. Formation of anatase titania occurred, in addition to the surface phase, at loadings in excess of 6 wt% Ti, with the amount of anatase increasing with Ti loadings. XRD analysis of TiO_2/Al_2O_3 revealed that segregation of crystalline anatase particles at a loading of 14 wt% Ti and the amount of crystalline anatase present was approximately 1.5 to 2 wt%, as estimated by XRD and LRS. Using the samples prepared from the grafting of silica with tetraisopropoxytitanium in isopropanol, Castillo *et al.* (21) reported that a very good dispersion of TiO_2 over silica (BET surface area of 320 $m^2 g^{-1}$) approaching monolayer dispersion was observed for TiO_2 content lower than about 15 wt%. At higher TiO_2 content, TiO_2 crystallites corresponding to octahedral coordination were formed. Lassaletta *et al.* (22) studied TiO_2 thin film prepared by evaporation of Ti in the presence of oxygen onto silica substrates. The supported titania phase showed a significant blue shift in its band gap observed by UV–VIS absorption spectra which was higher than the value expected based on the thickness of the TiO_2 layer. They ascribed such shifts to the fact that the coverage layer was constituted from TiO_2 crystallites smaller than the thickness of the deposited layer. These previous works are consistent with each other in TiO_2 forming a well-dispersed phase (surface or monolayer phase) at low Ti loadings and a crystalline TiO_2 at high loadings.

From the XRD results of Fig. 2, it was found that the titanium species in our TiO_2/SiO_2 catalysts was highly dispersed on silica support in agreement with previous reports discussed above. Below 5 wt% Ti loading, the titanium phase was not observed by XRD. The species in the catalysts seemed to be a highly dispersed Ti phase due to the strong interaction between silica and titanium(IV) dioxide. However, only the catalyst of 5 wt% Ti loading showed a single pre-edge peak of Ti *K*-edge XANES, the signature of a tetrahedral symmetry of Ti coordination although its spectrum represented a combined pre-edge peak of some fraction of octahedral Ti(IV) symmetry. The fine structure of postedge spectrum of 5 wt% sample is also distinguished from those of other spectra. Hence, this phase could be assigned as a surface phase of TiO_2 : SiO_2 forming a monolayer of TiO_2 on SiO_2 as in the case of TiO_2/Al_2O_3 (20).

At titanium loadings of 10 wt% and above, TiO_2 particles with the anatase structure is formed on SiO_2. This three-dimensional growth of titania is unequivocally manifested in XRD (Fig. 2) and XANES (Fig. 5) results. As more titanium is added above 10 wt%, the additional titanium contributes only to the growth of anatase particles and sharper XRD peaks are observed. XANES features, on the other hand, do not change as Ti loading increased above 10 wt% because the technique represents the local structure surrounding the absorbing atom (Ti) and is not sensitive to three-dimensional growth of the TiO_2 crystals.

Quantitative analysis of surface titanium measured by XPS is presented in Fig. 3. Rapid growth of surface Ti concentration below 5 wt% Ti loading suggests that most added titanium contributes to the monolayer formation. The slope of the surface Ti concentration vs Ti loading curve decreases above 5 wt% Ti loading and becomes flat from a Ti loading of 10–13 wt%. This shape of the curve could be interpreted as Ti added above 5 wt% contributing to the growth of both monolayer and bulk TiO_2 and then only to the three-dimensional growth above 10–13 wt% Ti loading.

Three characterization techniques of XRD, XANES, and XPS provide a consistent picture on the evolution of titanium structure in TiO_2/SiO_2 as the amount of titanium increased; a monolayer containing tetrahedral Ti(IV) at low Ti loadings and bulk TiO_2 crystals with anatase structure at high loadings. A simple calculation shows that a Ti loading of 14.5 wt% is needed to physically cover SiO_2 with a surface area of 300 $m^2 g^{-1}$ with a monolayer of tetrahedral TiO_2 species. Figure 3 suggests that monolayer coverage is reached around 10 wt% Ti loading and the amount of Ti actually used for monolayer should be less than 10 wt% because a part of it has formed three dimensional TiO_2 particles above 5 wt% Ti loading. Since the estimate assumes a complete close-packed coverage of whole SiO_2 surface with TiO_2, it would overestimate the amount of Ti required for a monolayer coverage. Hence, it could be concluded that agreement is reasonably good between estimation and observation of the saturation surface coverage.

It is interesting to see how this structural information could be related to the reactivity of TiO_2/SiO_2 in the gas phase transesterification of phenol and dimethylcarbonate. Figure 1 shows that phenol conversion shows a maximum at 10 wt% Ti loading. The selectivity to MPC increases first and becomes flat at 10 wt% Ti loading as the loading increased. The behavior of selectivity at increasing Ti loading is similar to that of surface Ti concentration shown in Fig. 3. The behavior of phenol conversion is also similar below 10 wt% loading. The results suggest that the surface titanium oxide is the active catalytic sites for the gas phase transesterification of phenol and dimethylcarbonate. Both monolayer and bulk TiO_2 appear to serve as active sites because the good MPC selectivity is maintained above 10 wt%. As mentioned, silica itself has a modest catalytic activity for the reaction showing phenol conversion of 14% and MPC selectivity of 52%. Thus the activity and selectivity of TiO_2/SiO_2 below 10 wt% loading should be combined contributions of surface TiO_2 and less active and less selective SiO_2. This accounts for the continued increase of MPC selectivity at low Ti loadings because added TiO_2 would cover the less selective SiO_2 surface.

Unlike selectivity to MPC, the conversion of phenol decreases as Ti loading goes above 10 wt%. This appears to be due to the decrease in surface area at the high loadings as

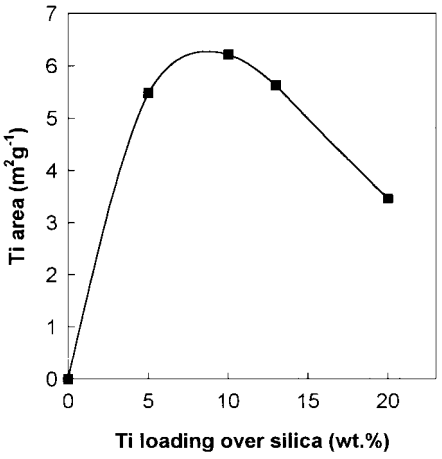

FIG. 7. The surface area of Ti obtained by the multiplication of the steady state BET surface area and the surface concentration of Ti by quantitative XPS analysis.

shown in Fig. 6. In order to demonstrate this point, the multiplication product of surface titanium concentration measured by XPS and BET surface area of used catalysts was plotted against Ti loadings in Fig. 7. The product should be proportional to the absolute amount of surface TiO_2 taking part in the catalytic reaction. The plot showed a remarkable resemblance with the curve of phenol conversion vs Ti loading. This supports our proposition that total surface titanium sites are responsible for the catalytic transesterification of phenol and dimethylcarbonate. The active Ti(IV) species are present in the forms of a monolayer and bulk crystals of the anatase structure or in tetrahedral and octahedral symmetries.

In Fig. 7, it is evident that the decrease in BET surface area is responsible for the reduced phenol conversions when Ti loading is increased above 10 wt%. As shown in Fig. 6, surface area of TiO_2/SiO_2 catalyst decreases as Ti loading is increased. However, the decrease in the surface area with Ti loading is not that great for fresh catalysts before the reaction. However, the decrease becomes much greater after the transesterification at 703 K for 8.5 h and thus the surface area difference between the fresh and used catalysts has become greater for higher Ti loadings. In a separate study to be published elsewhere, it has been found that the cause of the surface area reduction for used catalysts is coking (16). The presence of coke was confirmed by surface analysis with XPS, temperature-programmed reaction with H_2, and the measurement of pore-size distribution by N_2 adsorption. Thus, Fig. 6 indicates that coking is more favorable on catalysts with higher Ti loadings. Since these catalysts contain more bulk TiO_2 than catalysts with lower Ti loadings, it could be concluded that bulk TiO_2 promotes coking more effectively than monolayer Ti phase.

CONCLUSION

Silica-supported titania was the active catalyst for the synthesis of methylphenylcarbonate (MPC) from dimethylcarbonate (DMC) and phenol in the gas phase. The amount of surface Ti(IV) species highly dispersed due to a strong interaction of titania and silica increased with Ti loadings and got saturated above 10 wt%. This surface Ti(IV) species was directly responsible for the selective synthesis of MPC by the gas phase transesterification of DMC and phenol. The crystalline TiO_2 anatase phase was also an active and selective catalyst for gas phase transesterification, yet it also decreased the catalyst activity through the loss of surface area caused by coking.

ACKNOWLEDGMENT

This work has been supported by LG Chemicals Ltd. and Korean Science and Engineering Foundation through the Research Center for Catalytic Technology of Pohang University of Science and Technology.

REFERENCES

1. *Chem. Br.* **30**(12), 970 (1994).
2. Curtius, U., Bottoenbruch, L., and Schnell, H., U.S. patent 3 442 854 (1969).
3. Yamana, H., Kuni, T., Furusawa, T., Nakai, H., and Hiro, Y., U.S. patent 3 888 826 (1975).
4. Brunelle, D., U.S. patent 4 321 356 (1982).
5. Starr, J. B., and Ko, A., U.S. patent 4 383 092 (1983).
6. Komiya, K., Fukuoka, S., Aminaka, M., Hasegawa, K., Hachiya, H., Okamoto, H., Watanabe, T., Yoneda, H., Fukawa, I., and Dozono, T., *in* "Green Chemistry: Designing Chemistry for the Environment" (P. T. Anastas and T. C. Williamson, Eds.), p. 20. ACS, Washington, 1996.
7. Cusumano, J. A., *Chemtech* **22**(8), 482 (1992).
8. Fukuoka, S., Tojo, M., and Kawamura, M., U.S. patent 5 210 268 (1993).
9. Harrison, G. E., Dennis, A. J., and Sharif, M., U.S. patent 5 426 207 (1995).
10. Murata, K., Kawahashi, K., and Watabiki, M., U.S. Patent 5 380 908 (1995).
11. Fu, Z.-h., and Ono, Y., *J. Mol. Catal. A* **118**, 293 (1997).
12. Tundo, P., Trotta, F., Moraglio, G., and Ligorati, F., *Ind. Eng. Chem. Res.* **27**, 1565 (1988).
13. Kim, W. B., MS thesis, Pohang Univ. of Science and Technology, 1998.
14. Kim, W. B., and Lee, J. S., *Catal. Lett.*, in press.
15. Teo, B. K., "EXAFS: Basic Principles and Data Analysis." Springer, Berlin, 1985.
16. Kim, W. B., Kim, Y. G., and Lee, J. S., *Appl. Catal. A*, submitted for publication.
17. Bordiga, S., Coluccia, S., Lamberti, C., Marchese, L., and Zecchina, A., *J. Phys. Chem.* **98**, 4125 (1994).
18. Rhee, C. H., and Lee, J. S., *Catal. Today* **38**, 213 (1997).
19. Liley, P. E., Reid, R. C., and Buck, E., *in* "Perry's Chemical Engineers' Handbook" (R. H. Perry and D. Green, Eds.), 6th ed., Section 3, p. 276. McGraw-Hill, Singapore, 1984.
20. Stranick, M. A., Houalla, M., and Hercules, D. M., *J. Catal.* **106**, 362 (1987).
21. Castillo, R., Koch, B., Ruiz, P., and Delmon, B., *J. Catal.* **161**, 524 (1996).
22. Lassaletta, G., Fernandez, A., Espinos, J. P., and Gonzalez-Elipe, A. R., *J. Phys. Chem.* **99**, 1484 (1995).